Composites Science and Technology 74 (2013) 28–36

Contents lists available at SciVerse ScienceDirect

Composites Science and Technology

journal homepage: www.elsevier.com/locate/compscitech

Toughness distribution in complex PP/nanoclay injected mouldings

Valeria Pettarin [a,*], Florencia Brun [a], Julio C. Viana [b], Antonio S. Pouzada [b], Patricia M. Frontini [a]

[a] INTEMA Institute of Materials Science and Technology, University of Mar del Plata, A. Juan B. Justo 4302, B7608FDQ Mar del Plata, Argentina
[b] IPC/Institute for Polymers and Composites, University of Minho, Guimaraes Codex PT4800-058, Portugal

ARTICLE INFO

Article history:
Received 5 April 2012
Received in revised form 31 August 2012
Accepted 20 September 2012
Available online 28 September 2012

Keywords:
A. Nanoclays
A. Polymer–matrix composites (PMCs)
B. Fracture toughness
E. Injection moulding

ABSTRACT

The fracture performance of PP–nanoclay box-like injection mouldings obtained in double gated mould and by direct compounding of PP and a PP-based masterbatch was studied. Samples were observed by polarised light microscopy and characterised by DSC. Other samples were fractured using mode I double edge-notched tensile specimens. Their typically brittle fracture did not show neat in-plane crack propagation. The initial crack was branched and deviated out of the plane normal to the applied stress, and the fracture no longer followed the simple mode I. There is a tendency towards increasing the ductility and the deformation at break with the increase in nanoclay content. The fracture initiation does not depend on the nanoclay content or on the test piece location; nanoclay reinforcement increases the energy propagation release rate, G_{cp}, away from the weld line. The results allow the proposal of a model for the micromechanisms acting in samples which in-turn depends on nanoparticle orientation.

© 2012 Elsevier Ltd. All rights reserved.

1. Introduction

Propylene homo and copolymers (PP) are common materials for industrial automotive applications due to their many advantageous properties that include broad portfolio, low density, environmental stress-cracking resistance, unique ability to form integral hinges, price and ability to be readily recycled. Nonetheless, the application of pure PP in automotive is somewhat limited by its poor mechanical properties (such as tensile strength and impact resistance), scratch resistance or pre-treatment often required for painting [1].

In the last decade nanocomposites based on thermoplastics modified with nanoclays emerged as a topic of industrial and academic interest [2–4]. These nanocomposites have been reported to exhibit visible improvements when compared with the corresponding raw materials and micro- and macro-composites [5]. However it is been claimed that only well-dispersed and well-exfoliated nanoparticles can lead to the expected improvement of properties [6]. Raw material producers, converters and end-users have tackled both compounding and processing issues, usually resorting to the surface modification of nanofillers with organic surfactants and adaptation of compounding conditions to get rid of most of compounding issues. The development of masterbatches has reduced the health and safety hazards. The final injection or extrusion moulded parts may be easily obtained by mixing/diluting the masterbatch with the appropriate polymer matrix. The nanoparticle dispersion (and exfoliation where applicable) is usually assumed to be achieved during the masterbatch compounding.

Most PP-composites are processed by an injection moulding process. The injection moulding process involves the injection of a polymer melt flow into a mould impression where the melt cools and solidifies to form a plastics product. It is a three-phase process comprising filling, packing, and cooling. The occurrence of weldlines is a major design concern as weldlines could lead to a considerable reduction in mechanical properties; in consequence designers often need to incorporate liberal safety factors in design analysis to compensate for this weakness. Weldlines are often observed in injection moulded components due to multigate moulding, existence of pins, inserts, variable wall thickness and jetting and are classified as either being cold or hot. The cold weldlines are formed when two melt fronts meet head on and this type of weld provides the worst-case scenario as far as mechanical properties are concerned. While weld lines can be deleterious in homopolymer mouldings, the problem can be amplified in two-phase systems, such as reinforced thermoplastics [7]. For example, whilst the addition of spherical shaped fillers (e.g. glass spheres) has shown to have little effect upon tensile strength of injection moulded thermoplastics with weldlines, the addition of large aspect ratio fillers (e.g. short fibres) led to a considerable reduction in weldline strength due to the alignment of the fibres parallel to the weldline.

The understanding of the fracture, microdeformation and mechanics of nanocomposites is rather vague. Although claims are made that the mechanical properties of nanocomposites should be excellent, in practice the mechanical properties are often disappointing [8–12]. Cotterell and co-workers suggested that the orientation of the clay particles during injection moulding is

* Corresponding author. Tel.: +54 223 481 6600x183; fax: +54 223 481 0046.
E-mail addresses: pettarin@fi.mdp.edu.ar (V. Pettarin), jcv@dep.uminho.pt (J.C. Viana), asp@dep.uminho.pt (A.S. Pouzada), pmfronti@fi.mdp.edu.ar (P.M. Frontini).

0266-3538/$ - see front matter © 2012 Elsevier Ltd. All rights reserved.
http://dx.doi.org/10.1016/j.compscitech.2012.09.015

in part responsible for the embrittlement of semicrystalline polymers by nanoclay particles [13]. Much work has been done characterising injection moulded thermoplastic nanocomposite specimens [10,14–22]. However, as far as the authors know, there is no study of mechanical properties on actual PP–nanoclay mouldings, in which a complex orientation field and weld lines occur, and consequently it might be a distribution of properties.

In the case of the common mechanical properties such as the Young's modulus or the yield strength the testing techniques are simple and require little thought or interpretation. On the other hand, toughness is a more difficult property to characterise. In the past, the Izod or Charpy impact energies have been used to characterise toughness. In industry these types of tests continue to be used as an economical quality control method to assess the notch sensitivity and impact toughness of polymers. It has long been recognised that the impact energy is a complex strain rate function of the plastic and fracture work, the plastic work being generally dominating. The Izod and Charpy tests have lost favour in engineering design because they cannot be used directly in the calculations. In their desire to characterise toughness of ductile polymer nanocomposites more exactly, many researchers have turned to fracture mechanics (e.g. [13,23,24]).

Through this work it was studied the fracture performance of PP–nanoclay composite injection moulded parts obtained by direct compounding of a commercial PP and a PP based masterbatch (MB). A double gated mould was used, in which a weld line is formed by melt fronts meeting at different angles, and a distribution of molecules and particles orientation is generated from the injection points. The influence of singularities induced by flow pattern such as weld lines and injection points, as well as MB content on the arrangement of mechanical performance in the moulding were explored.

2. Experimental

2.1. Materials and processing

The study was conducted on propylene homopolymer, F-045 D2 (from Sunoco Chemicals) with MFI of 4.9 g/600 s at 230 °C, and a commercial MB of PP with 50% of organoclay, Nanomax-PP P-802 (from Nanomax Polyolefin Masterbatch Products).

The nanocomposites were obtained by direct injection of mixtures of PP and MB. Various amounts of nanoclay incorporation were used by mixing 2%, 6% and 10% of MB with PP, these mixtures being referred to hereon as PP-1, PP-3 and PP-5. Rectangular boxes of 1.4 mm thickness (Fig. 1) were injection moulded in a double-gated hot runner injection mould using a Klöckner Ferromatic FM20 injection machine with 200 kN clamping force. The processing setup is listed in Table 1.

2.2. Characterisation

2.2.1. Morphology

The global crystallinity of the material in the mouldings, that influences the mechanical properties, was determined after differential scanning calorimetry (DSC) tests on specimens that involve the whole skin–core structure. Tests were performed in a Perkin Elmer Pyris 1 device using 10 mg nominal sample weight, at a scanning rate of 10 °C/min from 50 °C to 200 °C under nitrogen atmosphere. The crystallinity was calculated as:

$$x_c = \frac{\Delta H}{(1-\phi)\Delta H^0} \tag{1}$$

where ΔH is the apparent enthalpy of fusion of the composite, ΔH^0 is the heat of fusion of 100% crystalline PP which is of 207.1 kJ/kg [25], and ϕ is the weight fraction of MB in the composites.15 μm-thick specimens were microtomed with a Leitz 1401 microtome and observed with an Olympus BH2 microscope using polarised light.

XRD analysis was performed on samples from the skin layer using a Phillips X'PERT MPD diffractometer (Cu Kα radiation λ = 1.5418 Å, generator voltage = 40 kV, current = 40 mA). Measurements were recorded every 0.02θ for 1 s each varying 2θ from 5° to 40°.

Scanning electron microscopy (SEM) was applied to observe cryofractured injection moulded specimens using JEOL JSM-6460 LV equipment

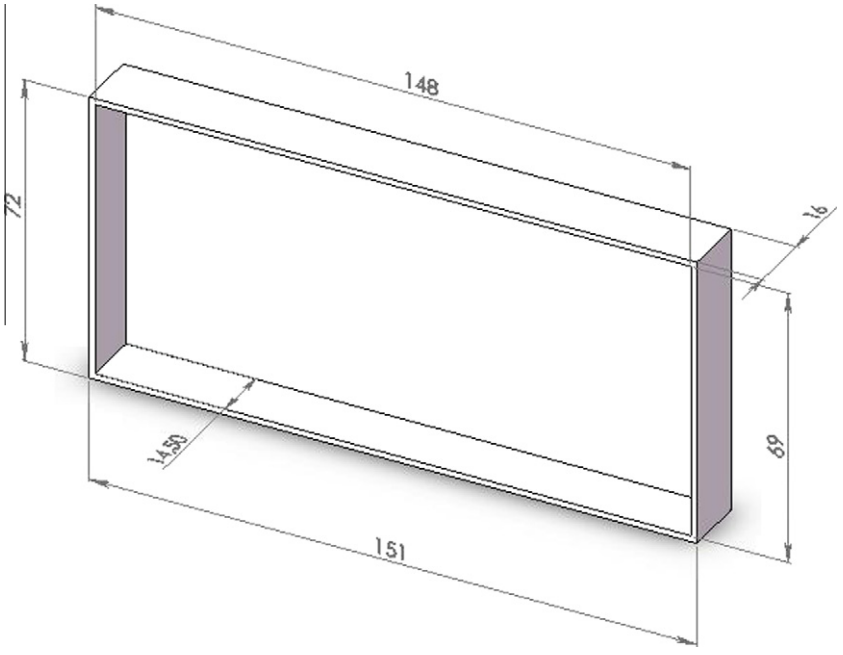

Fig. 1. Scheme of mouldings with their dimensions.

Table 1
Processing settings.

Processing parameter	Value
Injection temperature	235 °C
Mold temperature	60 °C
Screw rotation velocity	250 rpm
Injection rate	90.3 cm^3/s
Hydraulic packing pressure, time	300 kPa, 10 s
Back pressure	100 kPa
Cooling time	15 s

Transmission electron microscopy (TEM) microphotographs were obtained with a Jeol 100 CX microscope using an acceleration voltage of 200 kV. Samples were ultramicrotomed at room temperature with a diamond knife to a 70 nm thick section.

2.2.2. Fracture tests

Fracture characterisation was carried out on mode I double edge-notched tensile specimens (DENT) cut from the mouldings (nominal width, W, of 30 mm, nominal crack to depth ratio, a/W, of 0.5, and nominal length, S, of 70 mm), at a crosshead speed of 2 mm/min and room temperature in an Instron 4467 universal testing machine. Sharp notches were introduced by scalpel-sliding a razor blade having an on-edge tip radius of 13 μm with a Ceast Notchvis notching machine. In order to assess influence of the moulding singularities (as flow pattern and weld lines) in fracture, DENT samples were cut from different places of the mouldings as depicted in Fig. 2.

The initiation fracture toughness was evaluated as the stress intensity factor at 5% non-linearity [26]. The load at crack initiation F_q was determined as the intercept between the load curve and the $C+5\%$ compliance line, C being the initial compliance of the load–displacement curve. The stress intensity factor at initiation, K_{Iq} was then determined as:

$$K_{Iq} = \frac{F_q}{B\sqrt{\frac{W}{2}}} f\left(\frac{a}{W}\right) \tag{2}$$

where B is the thickness of the sample, W is the width of the sample, a is the length of the notch, and $f(a/W)$ is the function of the notch to width that for DENT samples is:

$$f\left(\frac{a}{W}\right) = \frac{\sqrt{\frac{\pi a}{2W}}}{\sqrt{1-\frac{a}{W}}}\left[1.122 - 0.561\left(\frac{a}{W}\right) - 0.205\left(\frac{a}{W}\right)^2 + 0.471\left(\frac{a}{W}\right)^3 + 0.19\left(\frac{a}{W}\right)^4\right] \tag{3}$$

In addition to the stress intensity factor at initiation, the propagation value of the strain energy release rate, G_{cp}, was estimated from the total fracture energy, U_{tot}, as [27]:

$$G_{cp} = \frac{U_{tot}}{B(W-a)}. \tag{4}$$

3. Results and discussion

3.1. Mouldings morphology

The typical skin–core structure of PP was found in the mouldings as revealed by polarised light microscopy (Fig. 3a). Skin thickness decreases with the increase in MB content (Fig. 3b) consistently with a reduction of PP macromolecules relaxation time and a higher shear dissipation induced by nanoclay particles [28]. The XRD patterns also indicated differences in the crystalline structure of the skin layer, as the intensities of the peaks corresponding to α-PP and β-PP phases change with nanoclay content (Fig. 4). However, the DSC data showed that the overall crystallin-

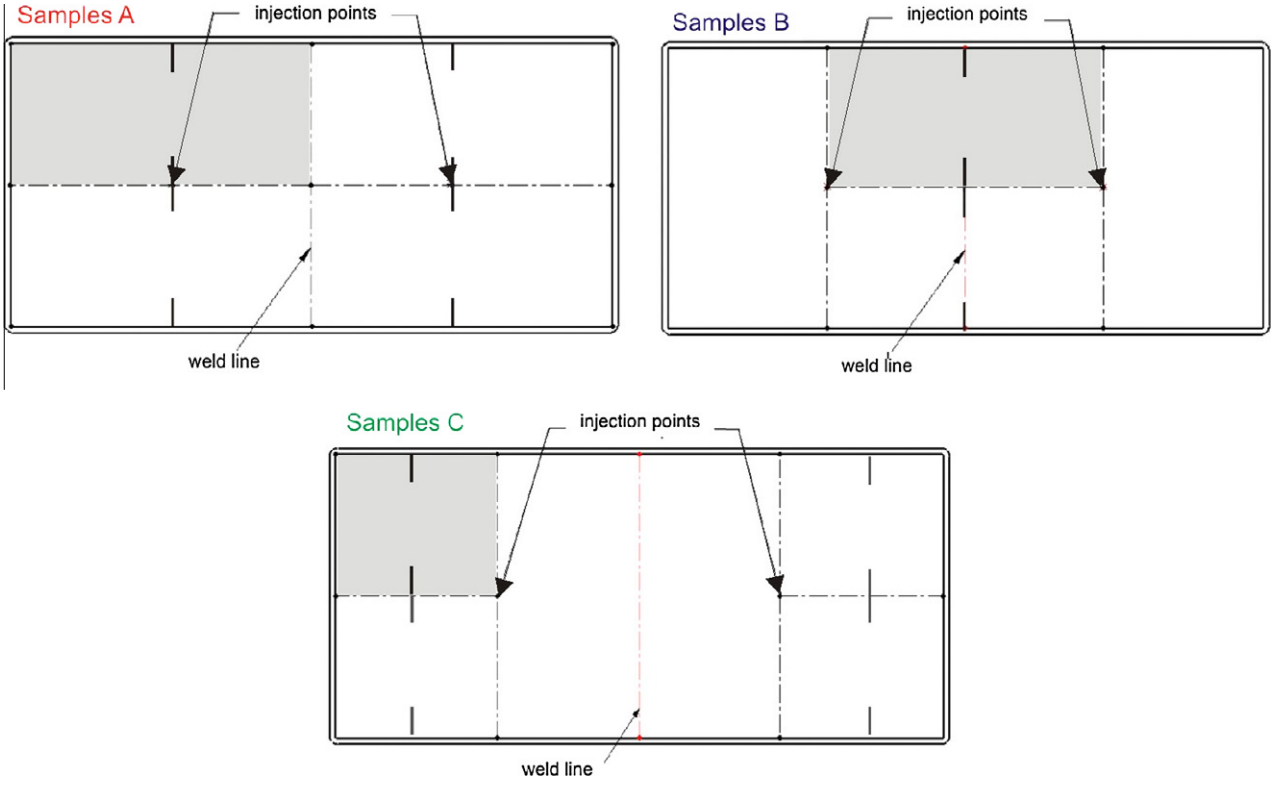

Fig. 2. Location of DENT samples. Type A samples: align with the injection point. Type B samples: in the weld line. Type C samples: away from the injection point.

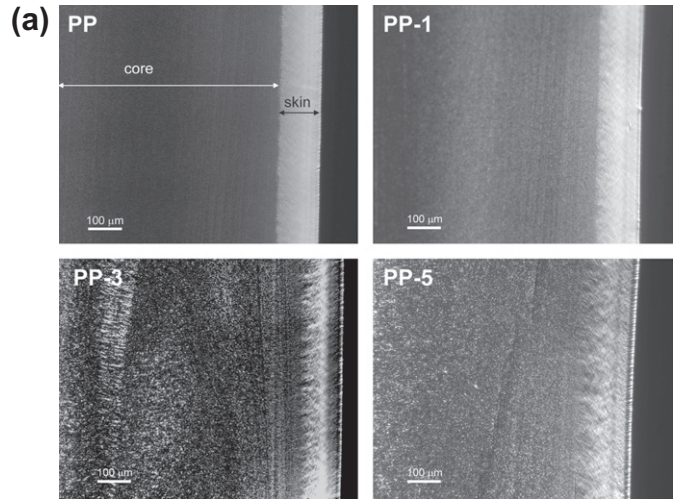

(b)

Material	Skin thickness (μm)
PP	97.8
PP-1	91.4
PP-3	86.9
PP-5	84.5

Fig. 3. Optical microscopy results (a) typical skin–core structure seen in mouldings (b) skin thickness as a function of MB content.

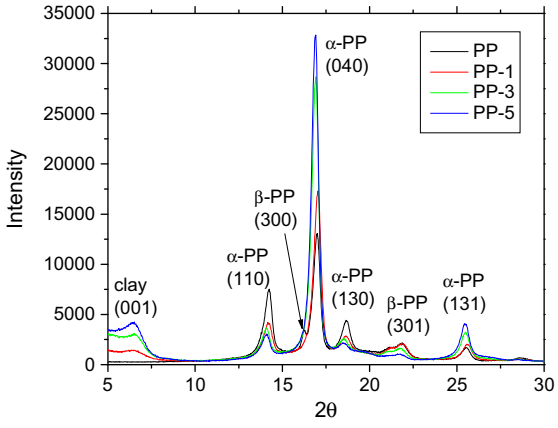

Fig. 4. XRD patterns of PP/nanoclay pieces.

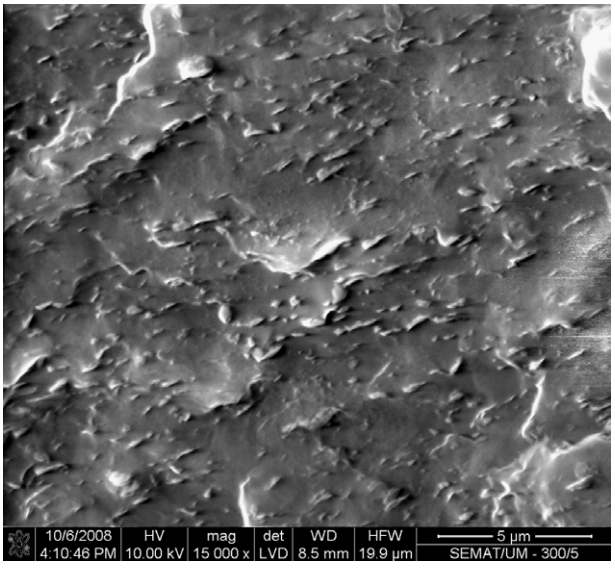

Fig. 6. Typical SEM picture of PP nanocomposites.

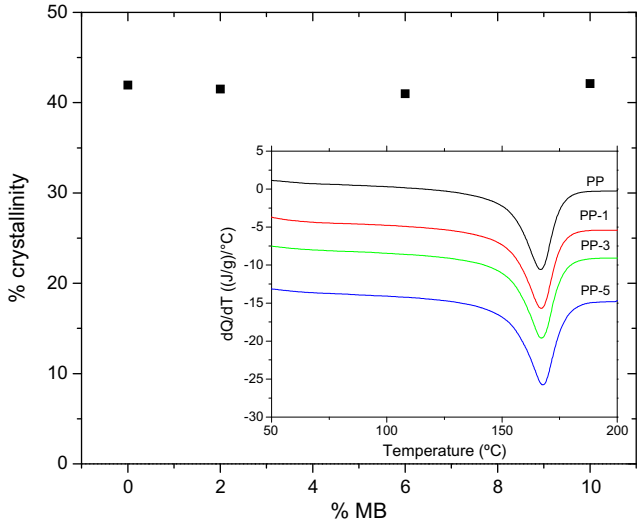

Fig. 5. DSC results: percentage of crystallinity as a function of MB content among with thermograms.

ity did not vary significantly with the amount of MB (Fig. 5). Further details of these analyses were already published elsewhere [28].

A good dispersion of nanoclay was achieved and no presence of aggregates was seen in the SEM pictures (Fig. 6). The XRD patterns indicate that the nanoclay platelets are not exfoliated, they are only intercalated (Fig. 4), and the stacked sheets clearly seen in TEM pictures (Fig. 7) confirm this finding. Even tough there is not much information about directly compound PP nanocomposites based on MB, our results of nanoclay dispersion and exfoliation are comparable to what is generally reported in the literature for these nanocomposites. Rajesh et al. [29] claimed that exfoliation does not occur during injection moulding leading to intercalated nanocomposites with a dispersion degree insufficient to achieve a percolation effect, in which clay platelets are dispersed as tactoids. Rodríguez-Llamazares et al. [30] also reported clays dispersed in the PP matrix in the form of small aggregates, similarly to our composites. These results indicate that the degree of nanoclay dispersion depends not only on the affinity and compatibility

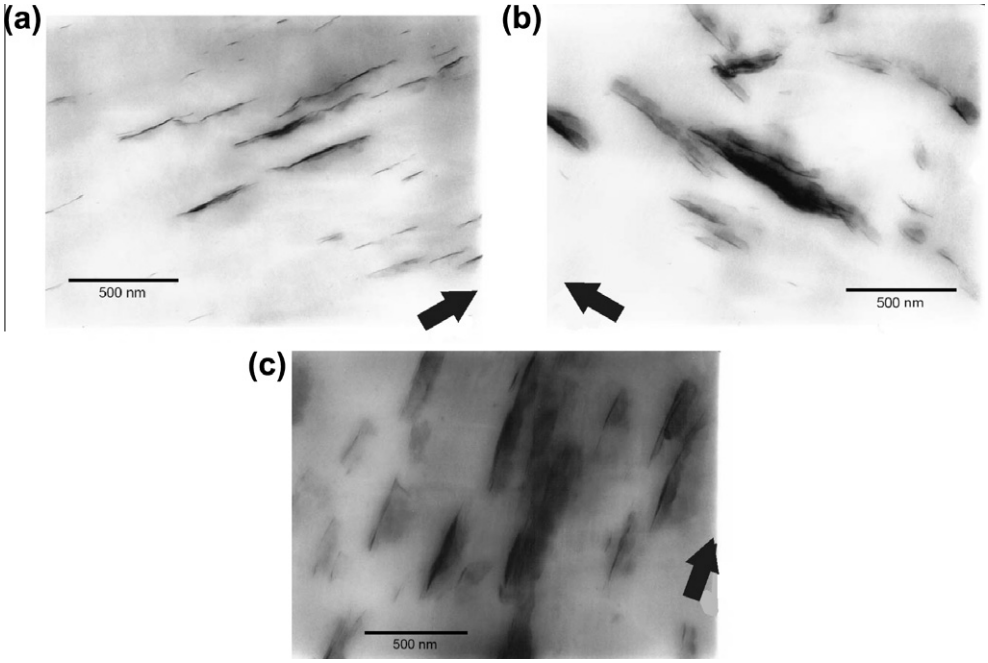

Fig. 7. TEM pictures of typical PP nanocomposites (arrows indicate flow direction). (a) PP-1. (b) PP-3. (c) PP-5.

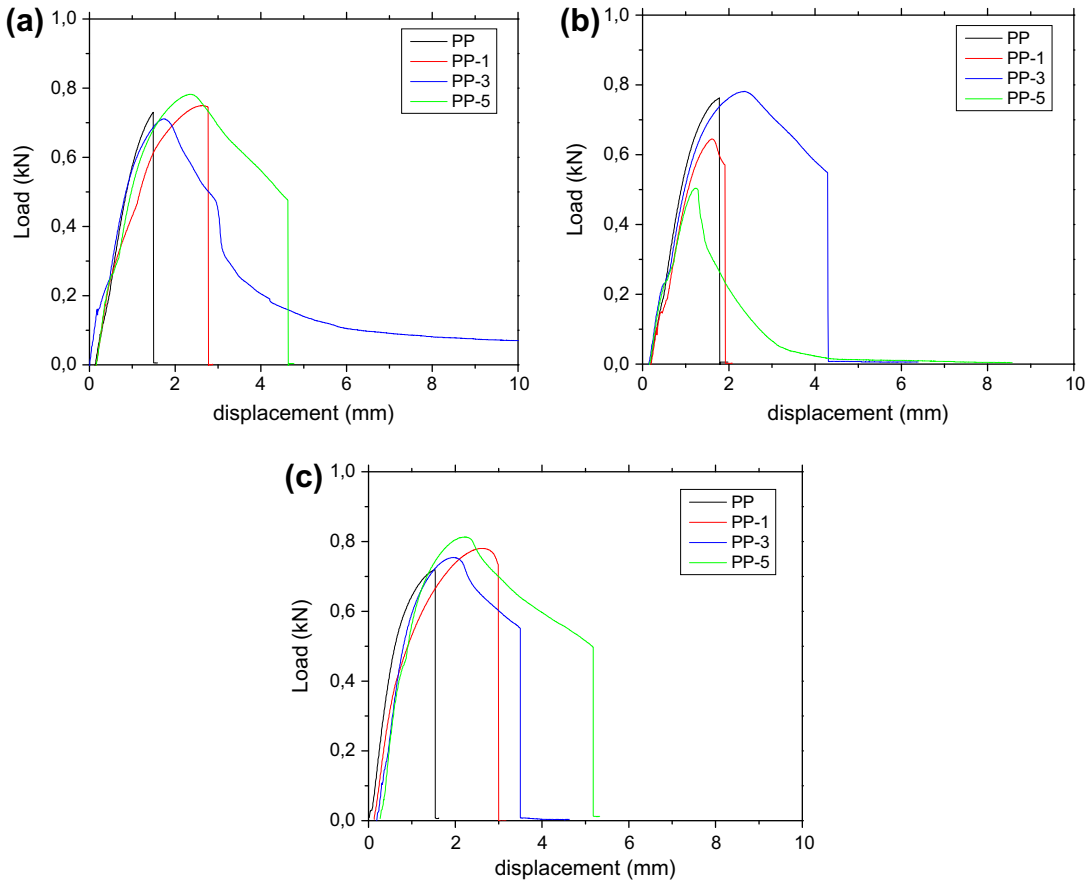

Fig. 8. Typical load–displacement curves for DENT samples. (a) Type A. (b) Type B. (c) Type C.

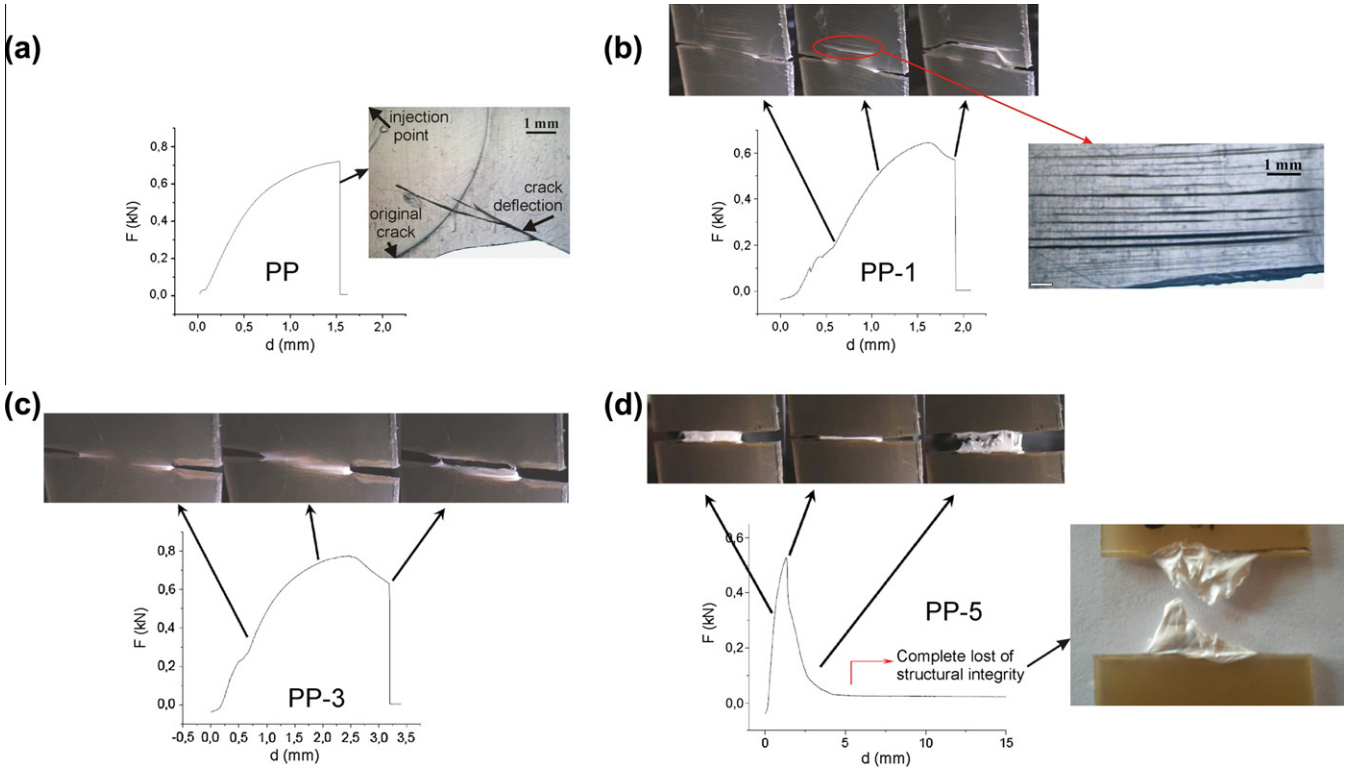

Fig. 9. Typical load–displacement curves and fracture development through the thickness. (a) PP. (b) PP-1. (c) PP-3. (d) PP-5.

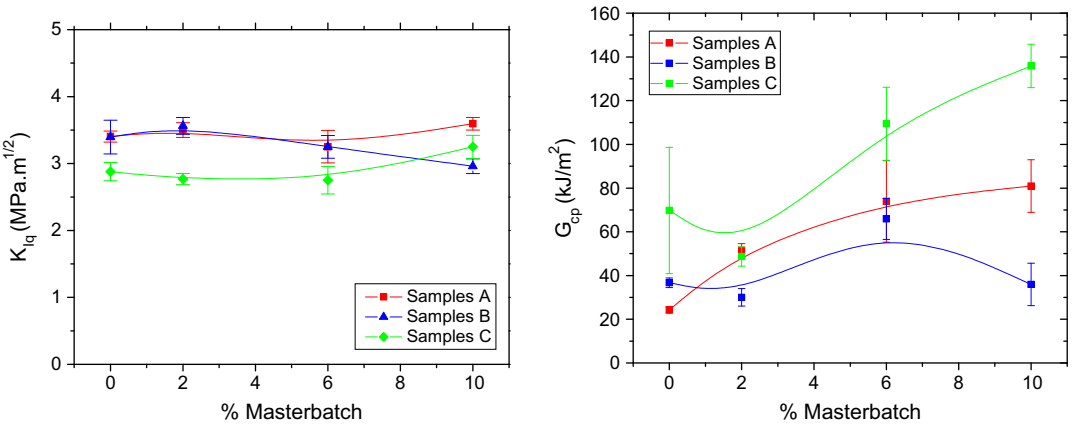

Fig. 10. Stress intensity factor at initiation and energy release rate for propagation in various places of the mouldings as a function of nanoclay content.

of the organoclay with the matrix (which is an intrinsic factor dependent on the material), but also on the shear stress (which is an extrinsic factor dependent on processing conditions and nanoclay loading) [31]. Hence, the incomplete organoclay exfoliation partially results from the imposed processing conditions not generating shearing enough to fully disperse the nanoclay agglomerates, although the MB suppliers claiming a gallery distance above 20 Å (Nanocor Technical Data).

3.2. Fracture behaviour

Typical stress–strain curves obtained at different places of the mouldings are shown in Fig. 8. PP samples underwent brittle fracture irrespective of their location in the moulding. The force fell almost instantaneously from the maximum to zero, indicating very low or nil propagation energy.

PP-1, PP-3 and PP-5 exhibit increasing ductile fracture characteristics, defined here as a fracture process that requires additional energy to propagate the crack through the specimen. A tendency toward increasing ductility and final propagation displacement was found in coincidence with the increase in MB content.

Further insight into the investigation of fracture performance can be acquired from the detailed inspection of the lateral views of the already tested DENT specimens. In Fig. 9 they are included typical examples of load–displacement curves for all materials together with pictures of the actual propagation of the fracture across the thickness and in the ligament region. It is clearly observed that PP behaved in a brittle manner and that the crack prop-

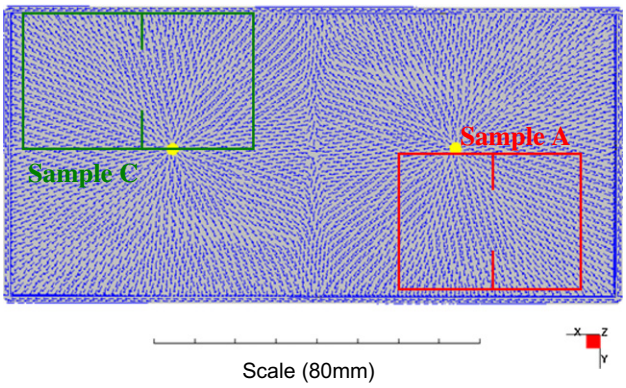

Fig. 11. Orientation field as simulated by moldflow.

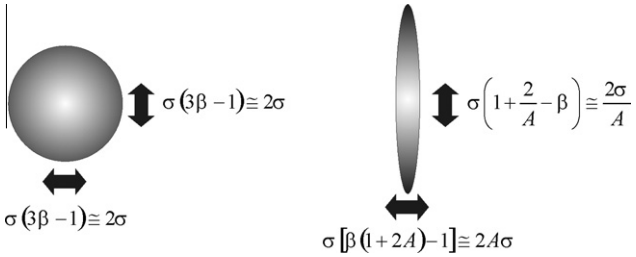

Fig. 12. Stress at the equator and pole of particles of different aspect ratio.

agated through the ligament of the specimen (Fig. 9a). However, these samples did not present neat in-plane crack propagation; the original crack was branched and deflected out of the plane that is normal to the applied uniaxial tensile stress meaning that the specimen was no longer loaded in simple mode I. In the nanocomposite mouldings, satellite cracks are visible in planes parallel to principal crack plane. In PP-1, in which the amount of ductile deformation is small, the coalescence of these satellite cracks provoked the deviation of the original crack out of the plane (Fig. 9b). This crack is no longer normal to the applied uniaxial stress meaning that the specimen was no longer loaded in simple mode I. Upon increasing the MB content (Fig. 9c and d), the ductility also increases (accompanied by the stress whitening of the ligament). However, side observation of these ductile-like samples show that skin and core underwent different deformations and failure mechanisms. The mid-thickness region, i.e. the core, underwent semi-brittle fracture with little contribution of plastic deformation. The external skin layers still connected the two halves of the specimen after the core fractured, and further increase in displacement was caused by elongation, necking and gradual fracture of the skin layers. Similar delamination between skin and core in injection moulded nanocomposites has been previously reported by other authors [16,32–34].

The initiation and propagation fracture toughness data are summarised in Fig. 10. It is clearly seen that the initiation fracture toughness depends neither on the nanoclay content nor the location in the mouldings. Unfortunately no improvements in toughness was seen in the weld line zone which remains as a weak zone.

However, a moderate toughening effect resulting from the nanoclay incorporation is seen in propagation fracture toughness of type A and C samples. There is a global tendency to believe that all composites' properties must be enhanced if the particle size is very small. Conversely, it has been found that intercalated layered silicates were more effective than exfoliated layered silicates in improving fracture toughness of nanocomposites [35]. Small particle size has a positive effect on many of the functional properties of polymer composites. However this is not completely true for toughness. There are many toughening mechanisms in composites which cannot be effective with nanoparticles. For example nanoparticles are too small to cause significant crack bridging or crack deflection. On the other hand the very large surface area of nanoparticles does provide the possibility of large energy absorption if they delaminate. However, even here there is an optimum particle size for toughening because the stress necessary to cause delamination is inversely proportional to the square root of the particle size [13]. According to Cotterel et al. statements, from a mechanical point of view there are two main potential sources of toughness in semicrystalline intercalated polymer nanocomposites: delamination or splitting of particles and matrix deformation where the major energy absorbing mechanism is the formation of multiple craze-like bands [13]. Both effects seem to be possible in our mouldings: there are intercalated particles that delaminate easier than fully exfoliated platelets, and PP can undergo multiple crazing. An interesting fact that should be taken into account is the toughening effect being more evident in type C samples than in type A samples. This trend may result both from geometrical aspects of the part and the mould filling pattern. Therefore it is useful to

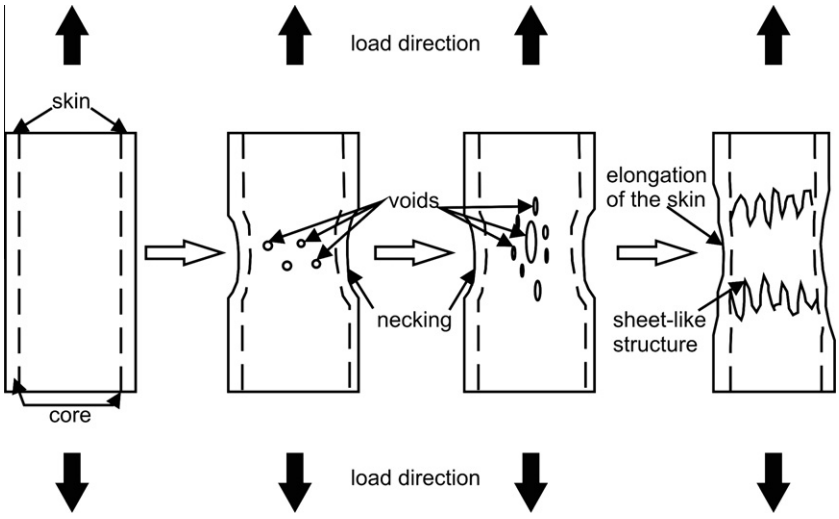

Fig. 13. Proposed micromechanical model of the fracture behaviour of PP nanocomposites.

recall here the uneven orientation of the polymer molecules in the mouldings (Fig. 11). Nanoclay platelets follow the flow orientation as it can be seen in Fig. 6 and 7 (for more evidence readers are referred to [28]). In type A samples nanoclay platelets are oriented parallel to the crack and may act as void-like defects inducing only little crazing and probably no delamination. On the other hand, in type C samples the nanoclay platelets are oriented approximated at 45° with relation to the crack line, and are more effective in initiating multiple crazes and particle delamination. This is easy to understand following the ideas of Cotterell and co-workers [13]. Near the tip of a notch the state of stress is near hydrostatic, but the stress in the loading direction will be a little larger. Under these conditions the stress at the equator and pole of a delaminated or voided spherical particle is given in Fig. 12 [36]. The stress around a spherical void is almost uniform and crazes can initiate anywhere around the void, whereas the stress at the equator of an ellipsoidal void is very much smaller than the stress at the pole. For example if the aspect ratio is 50, the then stress at the equator is only about 0.04σ, whereas the stress at the pole is about 100σ. Thus crazes can be readily initiated at the pole, but not at the equator and hence the development of multiple crazes.

3.3. A simple failure model proposal

Our interpretation of the failure mechanism in samples with adequate nanoparticle orientation is schematized in Fig. 13.

Cotterel and co-workers [13] stated that the delamination or splitting of nanoclay particles is a potentially significant source of toughness, this being related to the orientation of the nanoclay intercalated agglomerates with respect to the loading direction. In semi-crystalline polymers, like PP, shear yielding and craze-like bands are the mechanisms by which the matrix absorbs energy upon deformation. Nanosized free surfaces are necessary to initiate crazes and the delamination of clay particles produces those surfaces. Since it has been seen that crazes initiate only at the pole of nanoclay particles, only particles that due to flux are oriented at 45° or more can induce multiple crazing in tensile loaded samples and subsequently act as a toughening mechanism. This is further improved by the delamination of the nanoclay agglomerates.

During fracture, the stress field in the core is intensified by the thermal residual stresses generated during injection, e.g. [37,38]. Therefore cracks nucleate first in the core at sub-micron size particles and subsequently crazes appear perpendicularly to the direction of loading (Fig. 13b).

Due to the morphology differences between skin and core (mostly crystallite structure and molecular orientation), they may delaminate. Some of the crazes in the core develop as voids that grow in the load direction (Fig. 13c), producing the fracture of the core. This fracture develops as a sheet-like structure (Fig. 13d). Meanwhile the very oriented skin is still able to sustain load and to deform plastically (Fig. 13d).

The nanoclay toughening of polymers has been attributed to the local and global conformation of the polymers within the host galleries of nanoparticles being significantly different from that observed in the bulk. Assuming that the nanoclays are intercalated, this is due to the confinement of the polymer chain. An additional dissipative mechanism appears as a result of the mobility of the nanoparticles [39]. Since the nanofiller is interacting at the polymer chain level, the time scales for motion of both filler and polymer are comparable. As a result, during the deformation process the filler can create temporary polymer chain crosslinks, thereby creating a local region of enhanced strength and consequently retarding the growth of microdefects.

Our results suggest that the orientation induced by processing controls the toughness distribution in the injection mouldings.

4. Conclusions

Through this work fracture performance of PP/nanoclay injection moulded parts were obtained by direct compounding of a PP and a commercial MB, were studied. A double gated mould was used for generate a complex flow pattern inside the mould similar to typical mouldings. In these box-type mouldings a weld line is formed by melt fronts meeting at different angles, and a distribution of molecules and particles orientation is generated from the injection points. Thus, the influence of singularities induced by processing such as weld lines and injection point, as well as MB content on the arrangement of mechanical performance in the moulding could be explored.

PP mouldings at room temperature are typically brittle. Their fracture did not show a neat in-plane crack propagation as usually seen in simple mouldings. The initial crack was branched and deviated out of the plane normal to the applied uniaxial tensile stress following flow pattern, and consequently the fracture no longer followed the simple mode I.

In the PP nanocomposite mouldings a tendency towards increasing the ductility and the deformation at break were found in coincidence with the increase in MB content. Satellite cracks appeared and developed in planes parallel to the principal crack plane. However, ductile-like samples underwent semi-brittle fracture in the core, and the subsequent deformation resulted from elongation, necking and gradual fracture of the skin layers.

Regarding fracture toughness, the fracture initiation does not depend on the nanoclay content or on the test piece location. On the other hand, the nanoclay reinforcement increases the energy propagation release rate, G_{cp}, away from the weld line, as a result of the nanoclay content and the flow induced orientation.

Finally the results allowed the proposal of a model for the micro-mechanisms acting in samples with adequate nanoparticle orientation for toughening.

Acknowledgements

The authors thank the financial support of the National Research Council of Argentina (CONICET), the MINCyT (Argentina) and the FCT–Fundação para a Ciência e Tecnologia (Portugal) to this research.

References

[1] Karger-Kocsis J. Polypropylene: an A–Z reference. The Netherlands: Kluwer Academic Publishers; 1999.
[2] Alexandre M, Dubois P. Polymer-layered silicate nanocomposites: preparation, properties and uses of a new class of materials. Mater Sci Eng R: Rep 2000;28(1–2):1–63.
[3] Manias E, Touny A, Wu L, Strawhecker K, Lu B, Chung TC. Polypropylene/montmorillonite nanocomposites. Review of the synthetic routes and materials properties. Chem Mater 2001;13(10):3516–23.
[4] Paul DR, Robeson LM. Polymer nanotechnology: nanocomposites. Polymer 2008;49(15):3187–204.
[5] Zhang YQ, Lee JH, Rhee JM, Rhee KY. Polypropylene–clay nanocomposites prepared by in situ grafting–intercalating in melt. Compos Sci Technol 2004;64(9):1383–9.
[6] Krawczak P. Compounding and processing of polymer nanocomposites: from scientific challenges to industrial stakes. Express Poly Lett 2007;1(4):188.
[7] De SK, White JR. Short fiber–polymer composites. Cambridge (UK): Woodhead Publ. Ltd.; 1996.
[8] Pettarin V, Pontes A, Viau G, Viana J. Frontini PM, Pouzada A. Impact behavior of PP/nanoclay injection moldings. In: PPS 26th ann meeting, Banff, Canada; 2010.
[9] Pettarin V, Pita VJRR, Valenzuela-Díaz FR, Moschiar S, Fasce L, Seltzer R, et al. Preparation, physical and mechanical characterisation of montmorillonite/polyethylene nanocomposites. Key Eng Mater 2006;312:205–10.
[10] Pozsgay A, Papp L, Fráter T, Pukánszky B. Polypropylene montmorillonite nanocomposites prepared by the delamination of the filler. Progr Colloid Polym Sci 2001;117:120–5.

[11] Kornmann X, Thomann R, Mülhaupt R, Finter J, Berglund L. Synthesis of amine-cured, epoxy-layered silicate nanocomposites: the influence of the silicate surface modification on the properties. J Appl Polym Sci 2002;86(10):2643–52.
[12] Kinloch AJ, Taylor AC. Mechanical and fracture properties of epoxy/inorganic micro- and nano-composites. J Mater Sci Lett 2003;22(20):1439–41.
[13] Cotterell B, Chia JYH, Hbaieb K. Fracture mechanisms and fracture toughness in semicrystalline polymer nanocomposites. Eng Fract Mech 2007;74(7):1054–78.
[14] Tiwari RR, Paul DR. Polypropylene-elastomer (TPO) nanocomposites: 1 Morphology. Polymer 2011;52(21):4955–69.
[15] Tiwari RR, Paul DR. Polypropylene-elastomer (TPO) nanocomposites: 2. Room temperature Izod impact strength and tensile properties. Polymer 2011;52(24):5595–605.
[16] Saminathan K, Selvakumar P, Bhatnagar N. Fracture studies of polypropylene/nanoclay composite. Part II: Failure mechanism under fracture loads. Polym Test 2008;27(4):453–8.
[17] Baniasadi H, Ramazani SAA, Javan Nikkhah S. Investigation of in situ prepared polypropylene/clay nanocomposites properties and comparing to melt blending method. Mater Des 2010;31(1):76–84.
[18] Ferreira JAM, Reis PNB, Costa JDM, Richardson BCH, Richardson MOW. A study of the mechanical properties on polypropylene enhanced by surface treated nanoclays. Compos Part B: Eng 2011;42(6):1366–72.
[19] Wang K, Liang S, Zhao P, Qu C, Tan H, Du R, et al. Correlation of rheology–orientation–tensile property in isotactic polypropylene/organoclay nanocomposites. Acta Mater 2007;55(9):3143–54.
[20] Choi B-H, Chudnovsky A, Zhou Z. Observation of failure characteristics of notched injection molded pp/tpo/mmt nanocomposites. In: ICCE-17, Honolulu, Hawaii; 2009. p. 149–50.
[21] Zhou Y, Rangari V, Mahfuz H, Jeelani S, Mallick PK. Experimental study on thermal and mechanical behavior of polypropylene, talc/polypropylene and polypropylene/clay nanocomposites. Mater Sci Eng: A 2005;402(1–2):109–17.
[22] Perrin-Sarazin F, Ton-That MT, Bureau MN, Denault J. Micro- and nano-structure in polypropylene/clay nanocomposites. Polymer 2005;46(25):11624–34.
[23] Zerda AS, Lesser AJ. Intercalated clay nanocomposites: morphology, mechanics, and fracture behavior. J Polym Sci Part B: Poly Phys 2001;39(11):1137–46.
[24] Dunger S, Sandler JKW, Hedicke K, Altsadt V. Deformation and fracture behaviour of nanocomposites. In: Gdoutos EE, editor. Fracture of nano and engineering materials and structures. Netherlands; Springer: Springer; 2006. p. 93–4.
[25] Brandrup J, Immergut EH, Grukle EA. Polymer handbook. New York: Wiley; 1999.
[26] Williams JG. A linear elastic fracture mechanics (LEFM) standard for determining K_{Ic} and G_{Ic} for plastics. In: Moore CR, Pavan A, Williams JG, editors. Fracture mechanics testing methods for polymers, adhesives and composites, vol. ESIS Publication 28. The Netherlands: Elsevier; 2001.
[27] Adams MJ, Williams D, Williams JG. The use of linear elastic fracture mechanics for particulate solids. J Mater Sci 1989;24(5):1772–6.
[28] Pettarin V, Viau G, Fasce L, Viana JC, Pontes AJ, Frontini PM, et al. Impact behaviour of double-gated nanoclay-reinforced polypropylene injection mouldings. Polym Eng Sci, in press.
[29] Rajesh JJ, Soulestin J, Lacrampe MF, Krawczak P. Effect of injection molding parameters on nanofillers dispersion in masterbatch based PP–clay nanocomposites. Express Polym Lett 2012;6(3):237–48.
[30] Rodríguez-Llamazares S, Rivas BL, Pérez M, Perrin-Sarazin F, Maldonado A, Venegas C. The effect of clay type and of clay-masterbatch product in the preparation of polypropylene/clay nanocomposites. J Appl Polym Sci 2011;122(3):2013–25.
[31] Dennis HR, Hunter DL, Chang D, Kim S, White JL, Cho JW, et al. Effect of melt processing conditions on the extent of exfoliation in organoclay-based nanocomposites. Polymer 2001;42(23):9513–22.
[32] Uribe-Arocha P, Mehler C, Puskas JE, Altstädt V. Effect of sample thickness on the mechanical properties of injection-molded polyamide-6 and polyamide-6 clay nanocomposites. Polymer 2003;44(8):2441–6.
[33] Kwon HJ, Jar PYB. New energy partitioning approach to the measurement of plane-strain fracture toughness of high-density polyethylene based on the concept of essential work of fracture. Eng Fract Mech 2007;74(16):2471–80.
[34] Choi BH, Chudnovsky A, Zhou Z. Observation of failure characteristics of notched injection molded PP/TPO/MMT nanocomposites. In: ICCE-17, Honolulu, Hawaii; 2009. p. 149–50.
[35] Sun L, Gibson RF, Gordaninejad F, Suhr J. Energy absorption capability of nanocomposites: a review. Compos Sci Technol 2009;69(14):2392–409.
[36] Timoshenko S, Goodier JN. Theory of elasticity. New York: McGraw-Hill; 1951.
[37] Isayev AI, Crouthamel DL. Residual stress development in the injection molding of polymers. Polym–Plastics Technol Eng 1984;22(2):177–232.
[38] Zoetelief WF, Douven LFA, Housz AJI. Residual thermal stresses in injection molded products. Polym Eng Sci 1996;36(14):1886–96.
[39] Gersappe D. Molecular mechanisms of failure in polymer nanocomposites. Phys Rev Lett 2002;89(5):058301.